Assessment of combined electro-nanoremediation of molinate contaminated soil

Article *in* Science of The Total Environment · June 2014

DOI: 10.1016/j.scitotenv.2014.05.112 · Source: PubMed

5 authors, including:

Helena I Gomes
University of Nottingham

Eduardo P Mateus
Universidade NOVA de Lisboa

Celia Dias-Ferreira
Instituto Politécnico de Coimbra

Alexandra B. Ribeiro
Universidade NOVA de Lisboa

Assessment of combined electro-nano remediation of molinate contaminated soil

Helena I. Gomes[1,3], Guangping Fan [1,2], Eduardo P. Mateus[1], Celia Dias-Ferreira[3], Alexandra B. Ribeiro[1]

[1]CENSE, Departamento de Ciências e Engenharia do Ambiente, Faculdade de Ciências e Tecnologia, Universidade Nova de Lisboa, 2829-516 Caparica, Portugal

[2]Key Laboratory of Soil Environment and Pollution Remediation, Institute of Soil Science, Chinese Academy of Sciences (ISSCAS), East Beijing Road, Nanjing 210008, China

[3] CERNAS – Research Center for Natural Resources, Environment and Society, Escola Superior Agraria de Coimbra, Instituto Politecnico de Coimbra, Bencanta, 3045-601 Coimbra, Portugal

* Corresponding author. Tel. +351 212948300, Fax. +351 212948554. E-mail address: hrg@campus.fct.unl.pt (Helena I. Gomes)

ABSTRACT

Molinate is a pesticide widely used, both in space and time, for weed control in rice paddies. Due to its water solubility and affinity to organic matter, it is a contaminant of concern in ground and surface waters, soils and sediments. Previous works have showed that molinate can be removed from soils through electrokinetic (EK) remediation.

In this work, molinate degradation by zero valent iron nanoparticles (nZVI) was tested in soils for the first time. Soil is a highly complex matrix, and pollutant partitioning between soil and water and its degradation rates in different matrices is quite challenging. A system combining nZVI and EK was also set up in order to study the nanoparticles and molinate transport, as well as molinate degradation.

Results showed that molinate could be degraded by nZVI in soils, even though the process is more time demanding and degradation percentages are lower than in aqueous solution. This shows the importance of testing contaminants degradation, not only in aqueous solutions, but also in the soil-sorbed fraction. It was also found that soil type was the most significant factor influencing iron and molinate transport. The main advantage of the simultaneous use of both methods is the molinate degradation instead of its accumulation in the catholyte.

HIGHLIGHTS

- Molinate is degraded in soil by zero valent iron nanoparticles (nZVI)
- Higher contact time of nZVI with soil facilitates molinate degradation
- Soil type was the most significant factor influencing iron and molinate transport
- When using nZVI and EK molinate is degraded, not only transported to catholyte

KEYWORDS

Herbicide; nanoremediation; electrokinetics; contaminated soil; zero valent iron nanoparticles (nZVI)

1. Introduction

The widespread use of pesticides in intensive agriculture leads to soil and groundwater contamination. One of the pesticides that causes environmental concern is molinate (S-ethyl N,N-hexamethylene-1-carbamate), often applied annually to flooded fields during rice seeding to control the overgrowth of weeds (Castro et al., 2005). In 2013, there were 165.5 million hectares of rice paddies worldwide (FAO, 2013). Molinate can be found in natural surface and ground waters and also in wastewaters (Köck-Schulmeyer et al., 2013) due to its high water solubility (Table 1), as well as in soils and sediments near rice paddies (Castro et al., 2005; Cerejeira et al., 2003; Hildebrandt et al., 2007).

Zero valent iron nanoparticles (nZVI) degraded different pesticides in aqueous solutions, such as atrazine (Bezbaruah et al., 2009; Joo and Zhao, 2008; Satapanajaru et al., 2008), lindane (Elliott et al., 2009; Joo and Zhao, 2008), chloroacetanilide (Alachlor) (Bezbaruah et al., 2009) and molinate (Feitz et al., 2005), and remediated soils contaminated with pesticides such as malathion (Singhal et al., 2012), dinoseb (Satapanajaru et al., 2009), and chlorpyrifos (Reddy et al., 2013). Most of the research with iron nanoparticles analyzed the contaminants degradation in aqueous media, showing high degradation rates, including molinate degradation by nZVI through an oxidative process (Feitz et al., 2005; Joo et al., 2004). However, only a limited number of studies have assessed nanoparticle performance for soil-sorbed contaminants (Singh et al., 2012; Zhang et al., 2011), and as far as our knowledge concerns, no previous study was done for soil-sorbed molinate.

The combination of electrokinetic remediation (EK) and nZVI allows to enhance the transport of iron nanoparticles in low permeability fine-grain soils (Chowdhury et al., 2012; Gomes et al., 2013; Gomes et al.; Jones et al., 2010; Pamukcu et al., 2008; Rosales et al., 2014) and to degrade organic contaminants (Fan et al., 2013; Reddy et al., 2011; Yang and Chang, 2011; Yuan et al., 2012). With the simultaneous use of both remediation techniques

(EK and nZVI), the contaminant is not only removed from soil (traditional outcome in EK), but it is additionally degraded by nZVI, whose transport can also be enhanced by electric direct current. Electrokinetics can successfully remove molinate from soils to the catholyte due to electroosmotic transport as showed by Ribeiro et al. (2011), both by experimental work and modeling.

This work studies for the first time the degradation of molinate in soil using nZVI. It also assesses the integration of nZVI and electrokinetics to enhance the nanoparticles and molinate transport and degradation in two different soils.

2. Materials and Methods

2.1 Soils

We used two different soils: S1 (sandy), sampled near a sanitary landfill at Valadares, Vale de Milhaço, Portugal, and S2 (sandy loam with higher organic matter content), sampled in an industrial park, in central Portugal. Table 2 presents some of their physical and chemical characteristics.

2.2. Chemicals and solvents

Molinate standards were Pestanal grade, obtained from Riedel-de Haën (Seelze, Germany). The technical molinate (95%) used in the experiments was from Herbex (Sintra, Portugal). The solvents used in the present study were from Riedel-de Haën (Seelze, Germany), Panreac (Barcelona, Spain), Carlo Erba (Milan, Italy) and Merck (Darmstadt, Germany). Acetone was Gradient Grade, hexane was Pestanal grade, diethyl ether was ACS, methanol was HPLC grade and dichloromethane was SupraSolv grade. The water was distilled and purified with a Milli-Q plus system from Millipore (Bedford, MA, USA). The iron nanoparticles were in a slurry-stabilized suspension (NANOFER 25S, NANO IRON, s.r.o., Rajhrad, Czech Republic) negatively charged due to the coating with polyacrylic acid

(PAA), average particles size of 50 nm, average surface area of 20-25 $m^2 g^{-1}$, narrow particle size distribution of 20-100 nm and high iron content in the range of 80-90 wt. %.

2.3. Degradation tests

Both soils were spiked with technical molinate to obtain a final concentration of 290 mg kg^{-1}. After air-drying, 1 g of soil and 25 mL of deionized water and 200 µL of nZVI slurry (final concentration 1.0 g L^{-1} Fe) were placed in glass vials with a screw cap, in duplicate, under aerobic conditions, as the molinate degradation is an oxidative process (Joo et al., 2004). Blank samples were prepared as control, using the same spiked soil and without nZVI, for all the tested times. These soil suspensions were shaken in an orbital shaker (Bunsen A0 400) at 200 rpm at 25 ± 2ºC. After 24h, the samples were centrifuged for 10 min at 7500 rpm (Sorval RC5C Plus centrifuge). The supernatant was then removed and extracted through Solid Phase Extraction (SPE) using Strata X cartridges (200 mg/3mL; Phenomenex Torrance, CA, USA) on a vacuum rack. The molinate in the soil was extracted by 10 mL hexane after 20 min sonication (Bandelin Sonarex Super RK 102 H). The hexane extract was filtered through a 0.45 µm syringe Acrodisc PTFE filter (Pall Gelman Sciences, Ann Arbor, MI, USA) and concentrated under a gentle stream of nitrogen until 1.0 mL before analysis.

2.4. Electrokinetic experiments

2.4.1 Electrokinetic cell

The EK experiments were carried out in a laboratorial cell modified at the New University of Lisbon. The cell is divided into three compartments, consisting of two electrode compartments (L = 7.46 cm, internal diameter = 8 cm) and a central one (L = 4 cm, internal diameter = 8 cm), in which the soil, saturated with deionized water, is placed (Figure 1). This central compartment, made of Plexiglas, was equipped with an injection reservoir (L = 1 cm) for the iron nanoparticles, separated with 1 mm nylon mesh and a low speed filter paper. A set of five cellulose filters, previously tested and known to work as passive membranes

(Whatman filter paper), were used to separate the soil from the electrolytes. The soil section near the cathode is a non-spiked S1 soil in order to assess the molinate transport towards the cathode (Figure 1). A power supply (Hewlett Packard E3612A, Palo Alto, USA) was used to maintain a constant DC and the voltage drop was monitored (Kiotto KT 1000H multimeter). The electrodes were platinized titanium bars, with an L = 5 cm and a diameter of 3 mm (Bergsøe Anti Corrosion A/S, Herfoelge, Denmark). The fresh electrolyte was a 10^{-2} M $NaNO_3$ solution, with pH 7.0, and a peristaltic pump (Watson-Marlow 503 U/R, Watson-Marlow Pumps Group, Falmouth, Cornwall, UK) distributed it to the electrodes compartments. In all experiments, the electrolytes were collected into flasks and samples were analyzed.

2.4.2. Experimental conditions

Five different laboratory experiments (A–E) were carried out, according to the experimental conditions presented in Table 3. The variables considered were: i) the type of soil (two different soils with different texture, cation exchange capacity and organic matter content), ii) pH control as an EK enhancement method, and iii) absence of current as control experiments. No pH control experiment was made with soil S1 because its characteristics (sandy texture, low cation exchange capacity and low organic matter content) facilitate both molinate and nZVI transport.

The electrolyte used, in both anode and cathode compartments, was 10^{-2} M $NaNO_3$, with a flow rate of 1 mL min^{-1}. All experiments lasted 6 days (~145 h). A daily injection of 1 mL nZVI slurry – NANOFER 25S was made at the same time, after 10 min sonication, performing a total of 5 mL injected in each experiment. Electrolyte samples (catholyte and anolyte) were collected daily during the experiments, and their pH and volume were registered. At the end of each experiment, the total soil in the cell was sectioned into three "slices" and the center one was further divided into three (down, center and top) for iron and

molinate analysis. Subsamples were collected for humidity measurements. In experiments B and C, pH control was performed in the anolyte, through the manual addition of NaOH 1M, in order to keep the pH neutral (~7).

2.5. Iron analysis

The iron was extracted from soil by the sodium dithionite-citrate-bicarbonate (DCB) method (Mehra and Jackson, 1960) and from the electrokinetic cell and the membranes with concentrated hydrochloric acid. The iron analyses were made using Inductively Coupled Plasma-Atomic Emission Spectrometer (ICP) on a Horiba Jobin-Yvon equipment.

2.6 Molinate analysis

2.6.1. Aqueous samples: electrolyte solutions

The extraction of the molinate present in the electrolyte solutions was performed by SPE, using Strata X cartridges (500 mg/6 mL; Phenomenex, Torrance, CA, USA). The SPE cartridges were conditioned by washing with 2 × 3 mL of methanol, followed by 2 × 3 mL of Milli-Q water. The pH of the anolyte and catholyte daily samples was adjusted to values between 5 and 7, adding HCl or NaOH, before extraction. The aqueous samples were passed through the cartridge approximately at a flow-rate of 10 mL min^{-1} by applying a moderate vacuum. After that, the cartridges were washed with water and dried for approximately 1 min by vacuum. The analytes trapped in the cartridges were eluted sequentially with 2 × 2 mL of dichloromethane. The sample extracts were concentrated under a gentle stream of nitrogen to 1 mL. The samples were transferred to a vial and kept at −20ºC until GC analysis.

2.6.2. Solid samples: soils and passive membranes

Solid samples were extracted three times by sonication using 50 mL of methanol for 10 min to assure molinate maximum recovery. All the extracts were collected, as one and concentrated to 10 mL using 250 and 50 mL pear-shaped evaporating flasks on a rotary evaporator, Büchi RE 111 (35ºC/moderate vacuum). The concentrated extracts were

transferred to a Kuderna Danish concentrator tube and evaporated to approximately 5 mL. In order to remove the particulate matter, the extracts were filtered through 0.5 µm glass microfiber filters (MFV-5, 47 mm; Filter-Lab, Barcelona, Spain), prior to the concentration step, and through 0.2 µm syringe Chromafil PTFE filters (Macherey-Nagel, Duren, Germany) prior to the evaporation step.

2.6.3. Gas chromatography (GC)

Molinate analyses were performed by gas chromatography/mass spectrometry (GC/MS) on a HP5890 series II GC coupled to a HP5972 MSD (Hewlett-Packard, Palo Alto, California, USA). The column used was a ZB-5 (5%-phenyl 95%-dimethylpolysiloxane) with 30 m × 0.25 mm i.d. and 0.25 µm film thickness (Phenomenex, Torrance, CA, USA).

The oven temperature was programmed starting at 80ºC for 2 min, increased to 100ºC at a rate of 4ºC min^{-1} and then increased 8ºC min^{-1} to 250ºC, where it holds for 5 min. Helium was used as carrier gas at a flow rate of 1.0 mL min^{-1}. The injector was a split/splitless set at 250°C. The injections of 1.00 µl were performed at splitless mode (1 min) using an HP7673 autosampler (Hewlett-Packard, Palo Alto, California, USA).

The mass spectrometer was operated in the electron ionization mode (EI, 70 eV). The interface temperature was set at 280ºC and the EI source at 176ºC. Molinate analysis was carried out by full scan for identification (scan range 40–300 amu) and selected ion monitoring (SIM) for quantitative analysis using the base peak of molinate. The HP5972 MSD was tuned before analysis using PFTBA (perfluorotributylamine) as tuning standard. The data was registered and analyzed using ChemStation software (G1701BA, Version B.01.00).

3. Results and Discussion

3.1. Degradation tests

For both soils, the molinate concentrations in the supernatant are similar with and without iron nanoparticles. We would expect to find also identical concentrations in soils, but that does not occur (Figure 2), with molinate concentrations in soil being residual when iron nanoparticles are used. Comparing the molinate final amount in the experiments with and without nanoparticles (one-way analysis of variance – ANOVA), we found a significant difference for the concentrations of molinate in soils ($p < 0.01$). This supports the hypothesis that the iron nanoparticles degraded molinate added to the soil.

Molinate degradation occurs via an oxidative pathway that requires oxygen and the formation of hydrogen peroxide and hydroxyl radical (Joo et al., 2004). The degradation in aqueous solution can shift the molinate equilibrium between water and soil, facilitating molinate desorption from soil, and its subsequent degradation while in solution. We can also hypothesize that part of molinate degradation occurred during the centrifugation and the extraction of the soil samples. Iron nanoparticles were removed from the aqueous solution and were visible in the solid phase – here they remained in contact with the soil for about 30 to 45 minutes and molinate degradation could occur. Iron nanoparticles, because they are very strong reducing agents, are traditionally used for dechlorination of organochlorines (Elliott et al., 2008; Liu et al., 2005; Lowry and Johnson, 2004; Wang and Zhang, 1997). In reduction, the reaction occurs in the surface of the nanoparticles (Masciangioli and Zhang, 2003; Yan et al., 2013). However, in the oxidative pathway, the reaction is dependent on the formation of hydrogen peroxide and the hydroxyl radical, and only occurs in aerobic media, being consequently favored in the supernatant where molinate can more easily react with the hydroxyl radical.

A lower recovery of molinate was found in soil S2 (55±15%), when compared to recovery in soil S1 (76±17%), what may be related to its higher soluble organic matter content that, probably, overloaded the SPE columns that presented a dark brown colour after the extraction. Potential losses due to hydrolysis, biodegradation, photolysis and evaporation processes (Köck-Schulmeyer et al., 2013) can also contribute to this low recovery.

3.2 Electrokinetic experiments

3.2.1 Transport of iron nanoparticles

In all experiments, the aqueous solution in the anode compartment presented higher Fe concentrations than the one in the cathode compartment. In the majority of the catholyte samples, the iron concentrations were below the detection limit (100% of the samples in experiment A, 43% in experiment B, 86% in experiment C and 57% in experiment D, Table S2 in the Supplementary materials).

We measured the highest iron concentrations in the aqueous solutions in the diffusion experiments (D and E) and more specifically in the anode compartment, due to the lower distance from the injection reservoir (only 1 cm, Figures 1 and 3). A strong orange color and nanoparticles sedimentation in the anode compartment was visible in these diffusion experiments, which explains the peaks in the last segment of the cumulative Fe curves (Figure 3). This sedimentation did not occur in the cathode. Concerning the variable soil, we measured near the double of iron (16.24 mg vs. 8.38 mg) in the anolyte in experiment E (soil S1, sandy soil) when compared with experiment D (soil S2, loamy soil with high organic matter content). Similarly, more iron was found at the anolyte for experiment B (soil S1) than experiment C (soil S2). The difference in the soils texture contributes to this difference in transport. The sandy soil S1 will allow a faster transport of the iron nanoparticles, due to its higher pore volume (Gomes et al., 2013). Adsorption phenomena (Zhang et al., 2011) in soil particles and humic acid accumulation on the nZVI surface (Kim et al., 2013) most likely

hinder iron transport and this can also contribute to the lower iron concentrations in the anolyte in experiments with soil S2, when compared to those with soil S1 under similar operational conditions (Figures 3 and 4).

In the experiments with direct current (A, B and C), lower amounts of Fe were measured in the anolyte than in the diffusion experiments (D and E). Even though nanoparticles have a negative surface charge due to the polymer (PAA) coating, being expected to be electrophoretically transported towards the anode, electroosmotic flow generally occurs in the opposite direction (towards the cathode), and may hinder transport towards the anode, explaining lower concentrations found in the anolyte when direct current was applied. In the experiment with pH control (Exp. C, soil S2) 10 times more iron was, in average, found in the anolyte than in experiment A without pH control (soil S2), possibly because in this last case the advance of the acid front (H^+) oxidizes nanoparticles (Fe^0 ↝ Fe^{2+}), and the resulting positively charged iron ion is transported towards the cathode. However, only very small amounts of iron were measured in the catholyte in all experiments, probably because there was not enough time to reach the cathode compartment.

Comparing the amount of iron added and the remaining iron in the injection reservoir by the end of the experiments, the higher mobilization rate ($1 - C_f/C_0 \times 100$) was obtained for the experiment B (72%), followed by C (70%), E (62%), D (47%) and A (29%). The experiments with pH control (B and C) show an identical mobilization rate.

An analysis of variance (ANOVA) with the iron concentrations in the aqueous phase showed that the observed variance can be explained, at a 0.05 level, by the type of soil (S1 and S2) and the electric current (0 and 10 mA) (Table S1, Supplementary materials). The pH control was not significant to explain this variance.

In addition to iron in the electrolyte, its presence in the soil was also analyzed and compared to the initial content. Iron enrichment in the different soil slices is shown in Figure

4. Experiment A had more additional iron in the soil (Figure 4), followed by experiments D, C, B and E. This higher iron concentration in the soil in experiment A may be explained by the change of the soil charge with the advance of the acid front from the anode end due to the absence of pH control. In these conditions, ions of H^+ may adsorb to soil particles and increase the zeta-potential resulting in an increased adsorption of the PAA-coated iron nanoparticles. In all experiments, most of the iron was in the sections immediately after the injection reservoir. The section near the cathode (Section 5) presented the lowest amounts of additional iron (Figure 4), what is consistent with the concentrations found in the catholyte. This means that the iron accumulates in the nearest sections to the injection point. Nevertheless, no major differences existed in the three samples in the middle section (top, central and bottom) in experiments B, C and D, with relative standard deviation (RSD) of 9%, 6% and 5%, respectively; while in experiments A and E was higher (22% and 37%). There was no iron accumulation or deposition in the bottom part of this section (section 3), when compared to the central and top samples.

The mass balance of the iron shows that most of it stays in the injection reservoir of the cell, followed by the sum found in the soil and the passive membranes (Figure 5). This balance indicates a low mobility of the iron nanoparticles inside the experimental electrokinetic cell, most likely due to aggregation and sedimentation as also showed in other experimental setups with columns (Kocur et al., 2013; Phenrat et al., 2009; Saleh et al., 2008).

3.2.2. Transport and degradation of molinate

Our results confirm the transport of molinate towards the cathode with EK (Figure 6), as the experimental data and modeling by Ribeiro et al. (2011) showed. In the diffusion experiments (D and E) more molinate is found in the anode than in the cathode due to direct contact between molinate-spiked soil and the anode compartment, while at the cathode side a

non-contaminated soil layer is placed adjacent to the cathode compartment (Figures 1 and 6), hindering the appearance of molinate in the catholyte. Table 4 presents the electroosmotic transport of molinate towards the cathode, the diffusion towards the anode, the final content in the soils and its removal rate. Removal rate includes molinate transport from the soil and molinate degradation, calculated as the percentage of the quotient between the difference of the initial and final concentrations, and the initial concentration.

Previous studies have showed the strong adsorption of molinate in soils with high organic matter content (Alister et al., 2010) and this explains the 10-fold decrease in molinate in the anolyte of experiment D (soil S2, sandy-loam, 12.8% organic matter) when compared to experiment E (soil S1, sandy, 0.4% organic matter) (Figure 7).

The soil type is statistically significant to explain the molinate variance in the electrolyte (Table S1, Supplementary materials). Comparing the data of all experiments, the direct current and pH control are not statistically significant (p = 0.05) to explain molinate concentrations in the aqueous phase.

When an electric current is applied (experiments A, B, C) the amount of molinate in the anolyte decreases and molinate appears in soil section 5 (initially clean) near the cathode (Figure 7). This shows the electrokinetic transport of molinate towards the cathode. Once again, the higher amount of molinate in soil S2 (experiment C) compared to soil S1 (experiment B) can be explained by adsorption to soil organic matter, resulting in lower molinate removal efficiencies in these experiments (around 70% in B versus almost 90% in C).

The cumulative amounts of molinate found in the electrolyte (anolyte and catholyte) are less than 6% the initial amount in the soil (Table 4). In previous studies with EK but without nanoparticles (Santos, 2008), approximately 60% of the molinate was found in the catholyte, less than 2% in the anolyte and a maximum of 9% was found in soil. These

differences support the hypothesis that there was molinate degradation by nZVI in our experiments as, in identical conditions, fewer molinate was found in the electrolytes (catholyte).

The results now obtained show no enhancement in molinate degradation when both EK and nZVI are used, contrary to what was found for nitrates (Yang et al., 2008), dinitrotoluene (Reddy et al., 2011) and (Yuan et al., 2012). Although in those studies no diffusion tests were made, we must remark that the degradation rates are dependent on reduction reactions and molinate is degraded by nano Fe^0 via an oxidative pathway with hydroxyl radicals (Joo et al., 2004), not *via* the most common reductive pathway. This requires desorption of molinate and higher contact times than the reductive pathway. In our experiments, the diffusion tests were more effective for soil S2, most likely because EK, by transporting the molinate out of the system faster, reduced the contact times with iron nanoparticles. For soil S1 with lower resistance for molinate mobility, the applied direct current is not significant for its removal.

4. Conclusions

Results show that molinate degradation by zero valent iron nanoparticles via an oxidative pathway can also occur in soils. The soil-sorbed molinate degradation results show the importance of testing contaminants degradation with nZVI not only in aqueous solutions, but also in matrices increasingly more complex, such as synthetic groundwaters, real groundwaters, model soils and real soils. The degradation results in soils now obtained are much lower and more time demanding than in deionized water.

Soil type was the most significant variable for iron and molinate transport. In the tested conditions, iron moves preferentially to anode and molinate to cathode. Diffusion was the transport mechanism that yielded higher Fe concentrations in the anolyte. In the EK experiments, electrophoretic transport of iron nanoparticles was counteracted by

electroosmosis (higher in soil S2). For these experimental conditions, direct current was a significant variable to explain iron concentrations in the aqueous solutions, but it was not significant for molinate. In the tested conditions, there was no advantage in using the electric current to enhance the iron nanoparticles transport. We also observed limited mobility of the iron nanoparticles, with an average of 54% of the nanoparticles remaining in the injection reservoir.

Fe^0 nanoparticles and electrokinetics can degrade and remove molinate from soils, respectively. With electrokinetics, molinate can be removed from soil to an aqueous solution, and with nZVI molinate can be degraded *in situ*. The major advantage of the simultaneous use of both methods is the molinate degradation instead of its accumulation in the catholyte.

ACKNOWLEDGMENTS

This work has been funded by FP7-PEOPLE-IRSES-2010-269289-ELECTROACROSS, by Portuguese National funds through "Fundação para a Ciência e a Tecnologia" under projects PTDC/ECM/111860/2009 and PTDC/AGR-AAM/101643/2008 and by the research grant SFRH/BD/76070/2011. Carla Rodrigues from REQUIMTE is acknowledged for ICP analysis, and NANO IRON, s.r.o. for kindly providing NANOFER 25S samples.

REFERENCES

Alister CA, Araya MA, Kogan M. Adsorption and desorption variability of four herbicides used in paddy rice production. J Environ Sci Heal B 2010; 46: 62-68.

Bezbaruah AN, Thompson JM, Chisholm BJ. Remediation of alachlor and atrazine contaminated water with zero-valent iron nanoparticles. J Environ Sci Heal B 2009; 44: 518-524.

Castro M, Silva-Ferreira AnC, Manaia ClM, Nunes OC. A case study of molinate application in a Portuguese rice field: herbicide dissipation and proposal of a clean-up methodology. Chemosphere 2005; 59: 1059-1065.

Cerejeira MJ, Viana P, Batista S, Pereira T, Silva E, Valério MJ, et al. Pesticides in Portuguese surface and ground waters. Water Res 2003; 37: 1055-1063.

Chowdhury AIA, O'Carroll DM, Xu Y, Sleep BE. Electrophoresis enhanced transport of nano-scale zero valent iron. Adv Water Resources 2012; 40: 71-82.

Elliott DW, Lien H-L, Zhang W. Zerovalent iron nanoparticles for treatment of ground water contaminated by hexachlorocyclohexanes. J Environ Qual 2008; 37: 2192–2201.

Elliott DW, Lien HL, Zhang WX. Degradation of lindane by zero-valent iron nanoparticles. J Environ Eng 2009; 135: 317-324.

Fan G, Cang L, Qin W, Zhou C, Gomes HI, Zhou D. Surfactants-enhanced electrokinetic transport of xanthan gum stabilized nano Pd/Fe for the remediation of PCBs contaminated soils. Sep Purif Technol 2013; 114: 64-72.

FAO. Rice Market Monitor. XVI (3). Trade and Markets Division. Food and Agriculture Organization of the United Nations, 2013.

Feitz AJ, Joo SH, Guan J, Sun Q, Sedlak DL, David Waite T. Oxidative transformation of contaminants using colloidal zero-valent iron. Colloid Surf A 2005; 265: 88-94.

Gomes H, Dias-Ferreira C, Ribeiro A, Pamukcu S. Enhanced transport and transformation of zerovalent nanoiron in clay using direct electric current. Water Air Soil Poll 2013; 224: 1-12.

Gomes HI, Dias-Ferreira C, Ribeiro AB, Pamukcu S. Influence of electrolyte and voltage on the direct current enhanced transport of iron nanoparticles in clay. Chemosphere 2014; 99: 171-179.

Hildebrandt A, Lacorte S, Barceló D. Assessment of priority pesticides, degradation products, and pesticide adjuvants in groundwaters and top soils from agricultural areas of the Ebro river basin. Anal Bioanal Chem 2007; 387: 1459-1468.

Jones EH, Reynolds DA, Wood AL, Thomas DG. Use of electrophoresis for transporting nano-iron in porous media. Ground Water 2010; 49: 172-183.

Joo SH, Feitz AJ, Waite TD. Oxidative degradation of the carbothioate herbicide, molinate, using nanoscale zero-valent iron. Environ Sci Technol 2004; 38: 2242-2247.

Joo SH, Zhao D. Destruction of lindane and atrazine using stabilized iron nanoparticles under aerobic and anaerobic conditions: Effects of catalyst and stabilizer. Chemosphere 2008; 70: 418-425.

Kim D-G, Hwang Y-H, Shin H-S, Ko S-O. Deactivation of nanoscale zero-valent iron by humic acid and by retention in water. Environ Technol 2013; 34: 1-11.

Köck-Schulmeyer M, Villagrasa M, López de Alda M, Céspedes-Sánchez R, Ventura F, Barceló D. Occurrence and behavior of pesticides in wastewater treatment plants and their environmental impact. Sci Total Environ 2013; 458–460: 466-476.

Kocur CM, O'Carroll DM, Sleep BE. Impact of nZVI stability on mobility in porous media. J Contaminant Hydrol 2013; 145: 17-25.

Liu Y, Majetich SA, Tilton RD, Sholl DS, Lowry GV. TCE dechlorination rates, pathways, and efficiency of nanoscale iron particles with different properties. Environ Sci Technol 2005; 39: 1338-1345.

Lowry G, Johnson K. Congener-specific dechlorination of dissolved PCBs by microscale and nanoscale zerovalent iron in a water/methanol Solution. Environ Sci Technol 2004; 38: 5208-5216.

Mabury SA, Cox JS, Crosby DG. Environmental fate of rice pesticides in California. In: Ware G, editor. Reviews of Environmental Contamination and Toxicology. 147. Springer New York, 1996, pp. 71-117.

Masciangioli T, Zhang W. Environmental Technologies at the Nanoscale. Environ Sci Technol 2003; 37: 102A-108A.

Mehra OP, Jackson ML. Iron oxide removal from soils and clays by a dithionite-citrate system buffered with sodium bicarbonate. Clays Clay Miner. 1960; 7: 317-327.

Pamukcu S, Hannum L, Wittle JK. Delivery and activation of nano-iron by DC electric field. J Environ Sci Heal A 2008; 43: 934-944.

Phenrat T, Kim H-J, Fagerlund F, Illangasekare T, Tilton RD, Lowry GV. Particle size distribution, concentration, and magnetic attraction affect transport of polymer-modified Fe^0 nanoparticles in sand columns. Environ Sci Technol 2009; 43: 5079-5085.

Reddy AVB, Madhavi V, Reddy KG, Madhavi G. Remediation of chlorpyrifos-contaminated soils by laboratory-synthesized zero-valent nano iron particles: Effect of pH and aluminium salts. J Chem 2013; 2013: 1-7.

Reddy KR, Darko-Kagy K, Cameselle C. Electrokinetic-enhanced transport of lactate-modified nanoscale iron particles for degradation of dinitrotoluene in clayey soils. Sep Purif Technol 2011; 79: 230-237.

Ribeiro AB, Mateus EP, Rodríguez-Maroto J-M. Removal of organic contaminants from soils by an electrokinetic process: The case of molinate and bentazone. Experimental and modeling. Sep Purif Technol 2011; 79 193-203.

Rosales E, Loch JPG, Dias-Ferreira C. Electro-osmotic transport of nano zero-valent iron in Boom Clay. Electrochimica Acta 2014; 127: 27-33.

Saleh N, Kim H-J, Phenrat T, Matyjaszewski K, Tilton RD, Lowry GV. Ionic strength and composition affect the mobility of surface-modified Fe^0 nanoparticles in water-saturated sand columns. Environ Sci Technol 2008; 42: 3349-3355.

Santos JCS. Electrokinetic remediation of rice field soils contaminated by molinate, Dissertação de Mestrado, Faculdade de Ciências e Tecnologia da Universidade Nova de Lisboa, 97 pp.

Satapanajaru T, Anurakpongsatorn P, Pengthamkeerati P, Boparai H. Remediation of Atrazine-contaminated Soil and Water by Nano Zerovalent Iron. Water Air Soil Poll 2008; 192: 349-359.

Satapanajaru T, Onanong S, Comfort SD, Snow DD, Cassada DA, Harris C. Remediating dinoseb-contaminated soil with zerovalent iron. J Hazard Mater 2009; 168: 930-937.

Singh R, Misra V, Mudiam MKR, Chauhan LKS, Singh RP. Degradation of HCH spiked soil using stabilized Pd/Fe^0 bimetallic nanoparticles: Pathways, kinetics and effect of reaction conditions. J Hazard Mater 2012; 237-238: 355-364.

Singhal RK, Gangadhar B, Basu H, Manisha V, Naidu GRK, Reddy AVR. Remediation of malathion contaminated soil using zero valent iron nano-particles. Am J Anal Chem 2012; 3: 76-82.

Wang C-B, Zhang W. Synthesizing nanoscale iron particles for rapid and complete dechlorination of TCE and PCBs. Environ Sci Technol 1997; 31: 2154-2156.

Yan W, Lien H-L, Koel BE, Zhang W-x. Iron nanoparticles for environmental clean-up: recent developments and future outlook. Environ Sci: Processes Impacts 2013; 15: 63-77.

Yang GCC, Chang Y-I. Integration of emulsified nanoiron injection with the electrokinetic process for remediation of trichloroethylene in saturated soil. Sep Purif Technol; 79: 278–284.

Yang GCC, Hung C-H, Tu H-C. Electrokinetically enhanced removal and degradation of nitrate in the subsurface using nanosized Pd/Fe slurry. J Environ Sci Heal A 2008; 43: 945-951.

Yuan S, Long H, Xie W, Liao P, Tong M. Electrokinetic transport of CMC-stabilized Pd/Fe nanoparticles for the remediation of PCP-contaminated soil. Geoderma 2012; 185-186: 18-25.

Zhang M, He F, Zhao D, Hao X. Degradation of soil-sorbed trichloroethylene by stabilized zero valent iron nanoparticles: Effects of sorption, surfactants, and natural organic matter. Water Res 2011; 45 2401-2414.

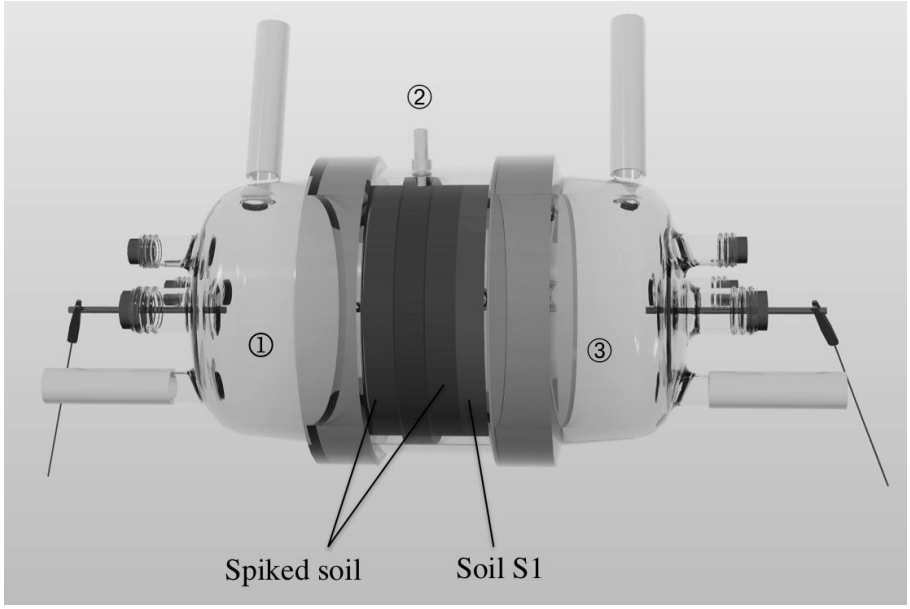

Figure 1. Schematic representation of the laboratory cell. Legend: ① Anode compartment; ② Reservoir for the iron nanoparticles injection; ③ Cathode compartment. The separation between the soil and the compartments containing liquids was made through passive membranes (filter paper).

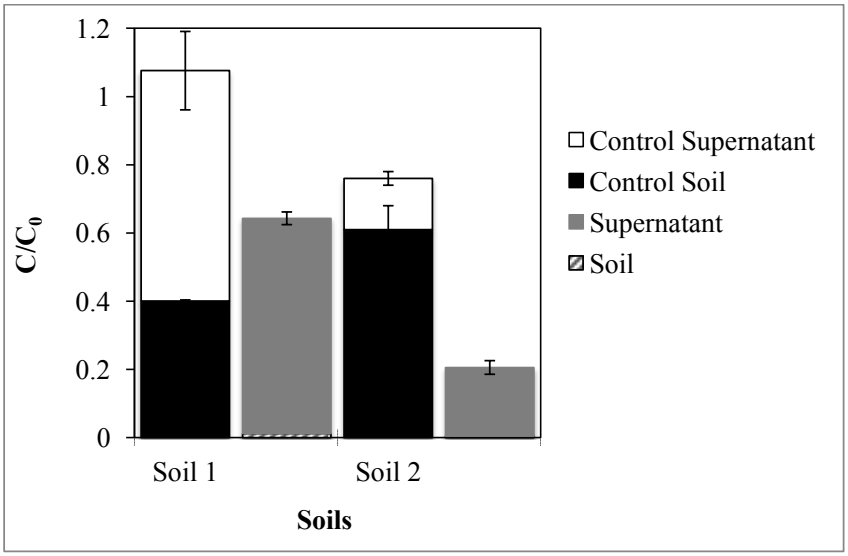

Figure 2. Molinate concentrations in the soil and supernatant after 24 h, with and without nZVI (control) in S1 sandy soil and S2 sandy-loam soil. Initial molinate concentration in soil was 290 mg kg^{-1}. Data plotted as mean of duplicates, error bars indicate standard deviation.

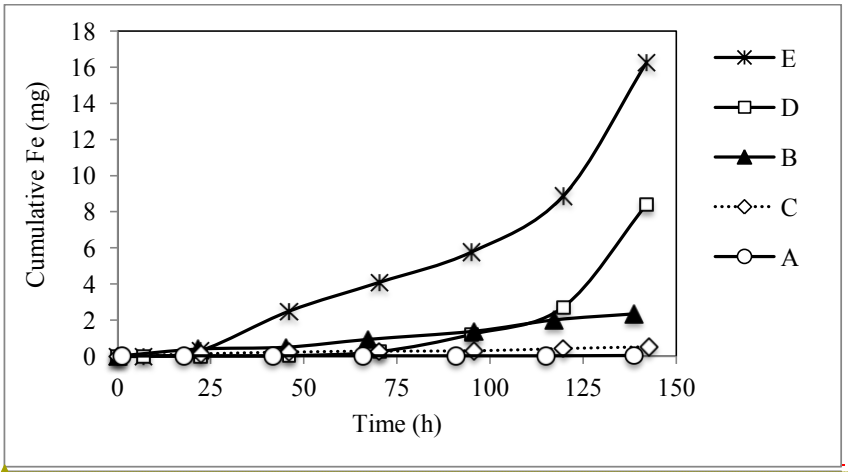

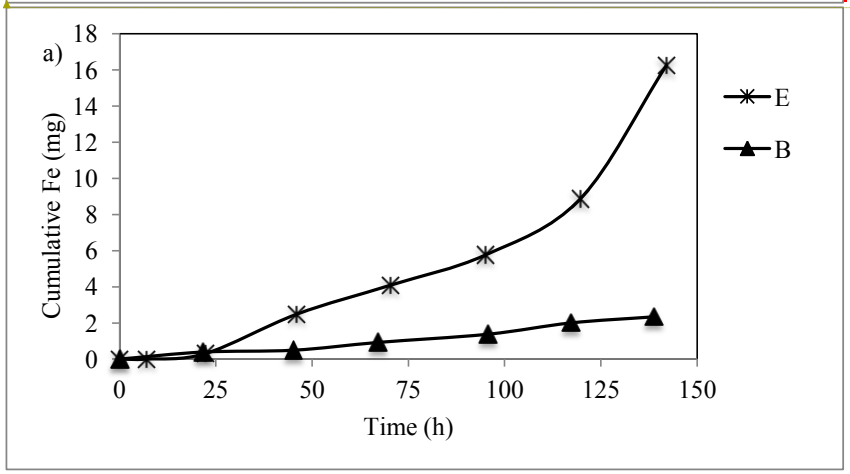

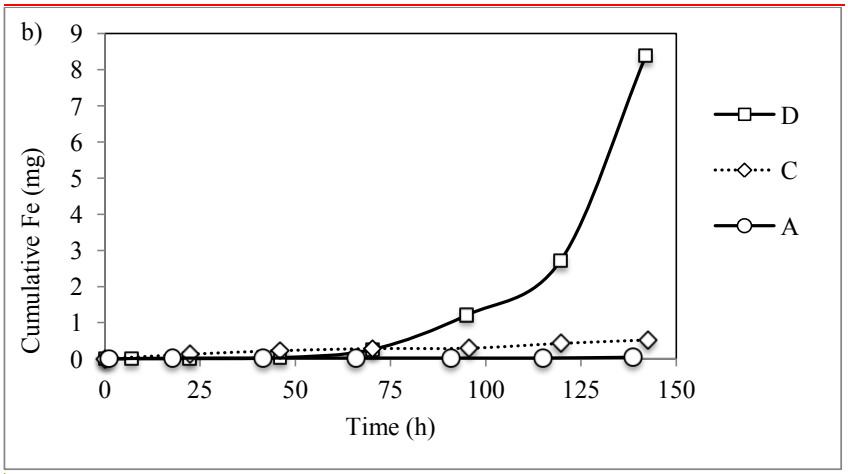

Figure 3. Cumulative amounts of total iron (mg) in the anolyte solutions during the experiments ~~A (Soil 2, no pH control)~~. a) Experiments with soil 1 (sandy soil): B (~~Soil 1,~~EK with pH control) and E (diffusion);
b) Experiments with soil 2 (sandy loam with high organic matter content): A (EK without pH control), C (~~Soil 2,~~EK with pH control~~), D (Soil 2, diffusion~~) and ~~E (Soil 1,~~ D (diffusion). In the cathode compartment, iron was detected in very low concentrations and in most of the samples was ~~bellow~~below the detection limit.

Formatted: Font: Times

Formatted: Font: Times

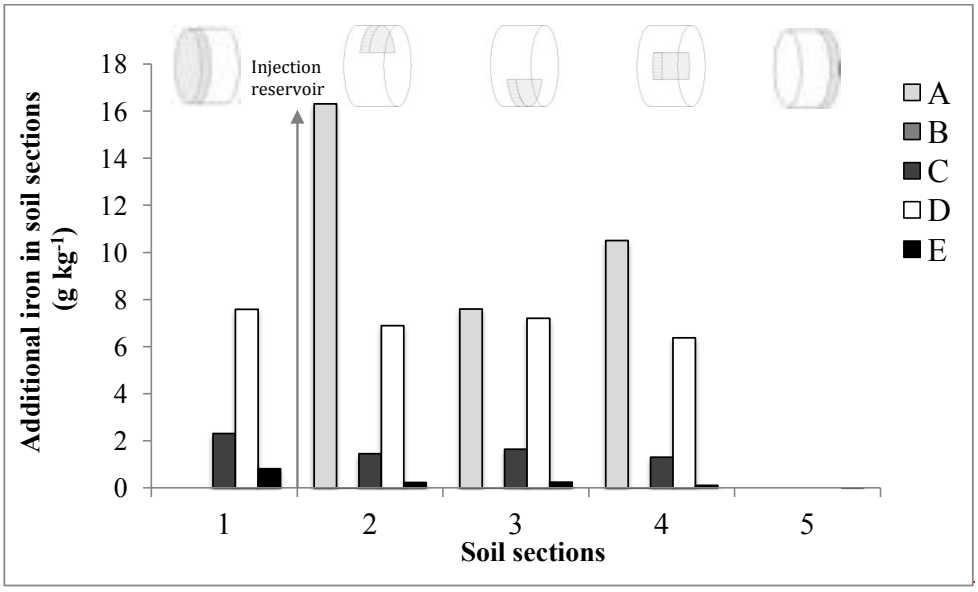
Injection reservoir
Additional iron in soil sections (g kg-1)
18
16
14
12
10
8
6
4
2
0
1
2
3
4
5
Soil sections
A
B
C
D
E

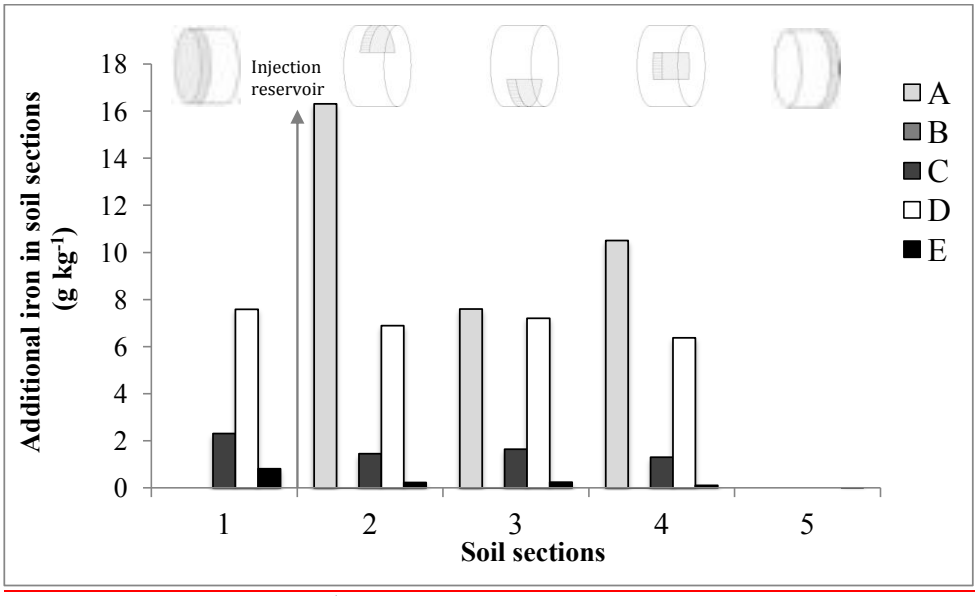

Figure 4. Iron enrichment (g kg^{-1}) in soil sections (compared to initial soil concentration: 18.43 g kg^{-1} in Soil S1 and 0.85 g kg^{-1} in Soil S2) in experiments A-E. Section 1: between the anode compartment and the injection reservoir; Section 2: central soil section after the injection reservoir, top; Section 3: central soil section after the injection reservoir, bottom; Section 4: central soil section after the injection reservoir, center; Section 5: between the central soil section and the cathode compartment.

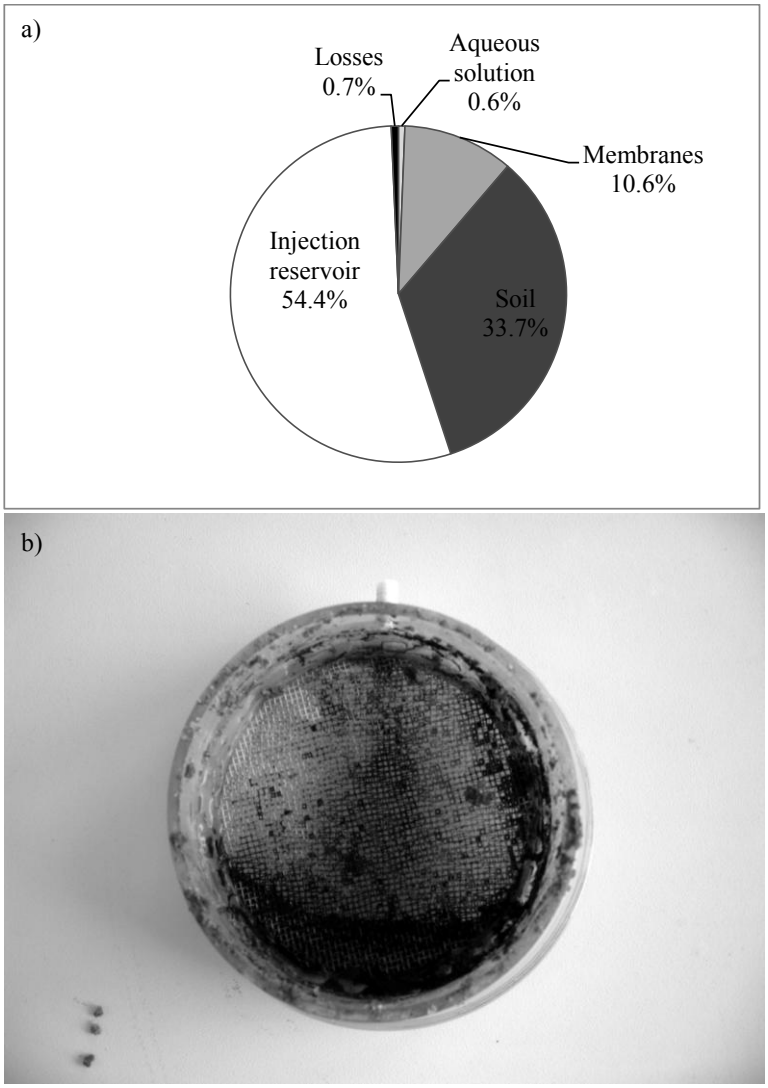

Figure 5. a) Average mass balance of iron after the experiments. Average recovery of iron was 86%. b) Photo of the experimental cell showing the iron accumulation in the injection reservoir.

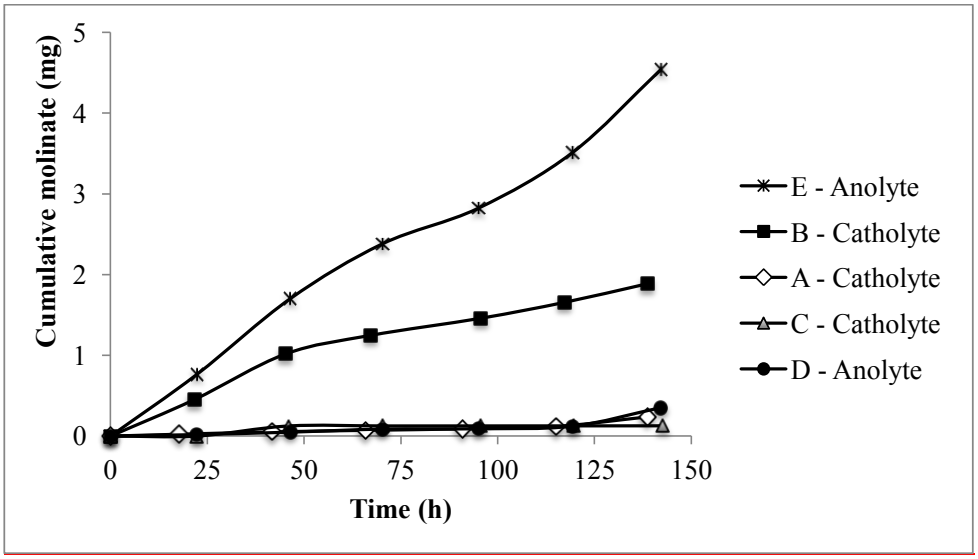
Cumulative molinate (mg)
Time (h)
E - Anolyte
B - Catholyte
A - Catholyte
C - Catholyte
D - Anolyte

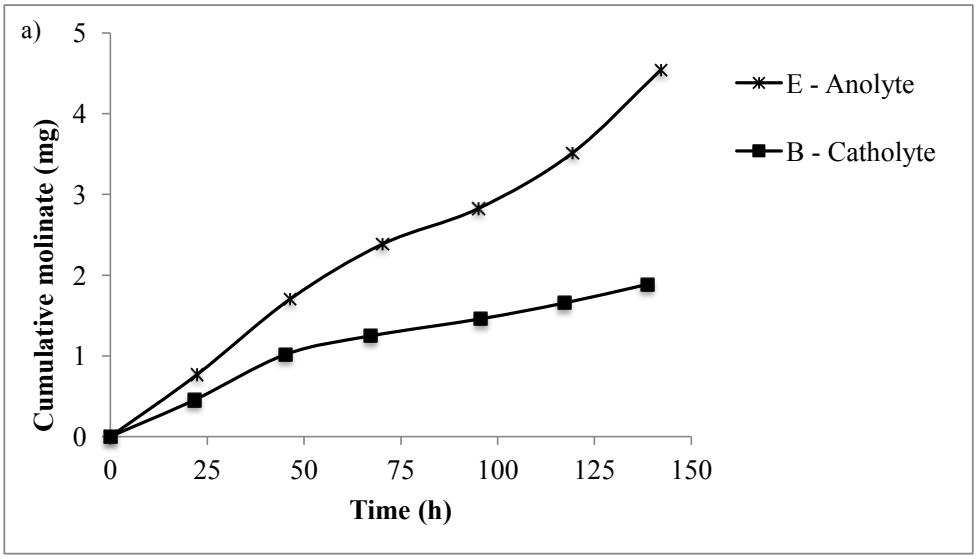
a)
Cumulative molinate (mg)
Time (h)
E - Anolyte
B - Catholyte

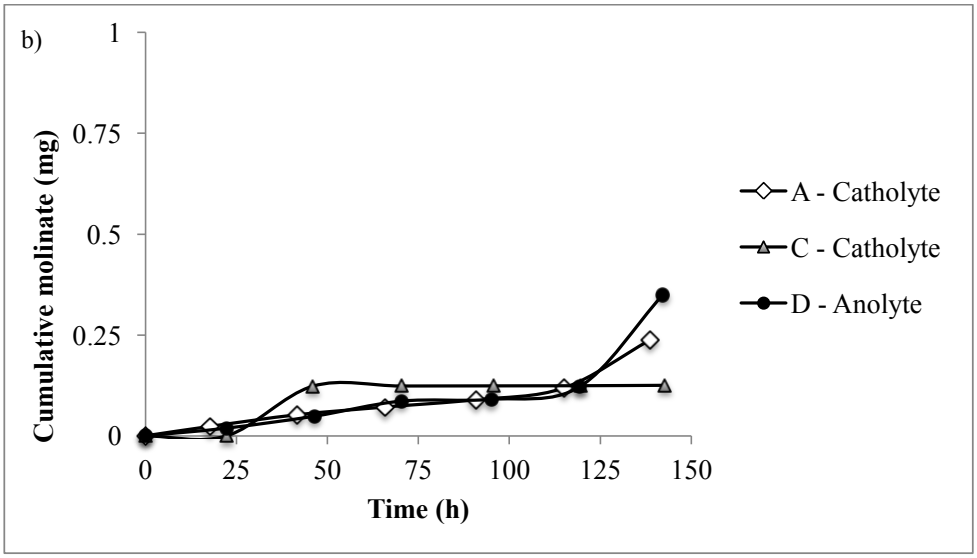

Figure 6. Cumulative amounts of molinate (mg) in the anolyte and catholyte solutions during the experiments ~~**A (Soil 2, no pH control), B (Soil 1, with pH control) and C (Soil 2, with pH control), D (Soil 2, diffusion) and E (Soil 1, diffusion). In the diffusion experiments higher molinate content was found in the anolyte due to the direct contact with the spiked soil**~~**.**

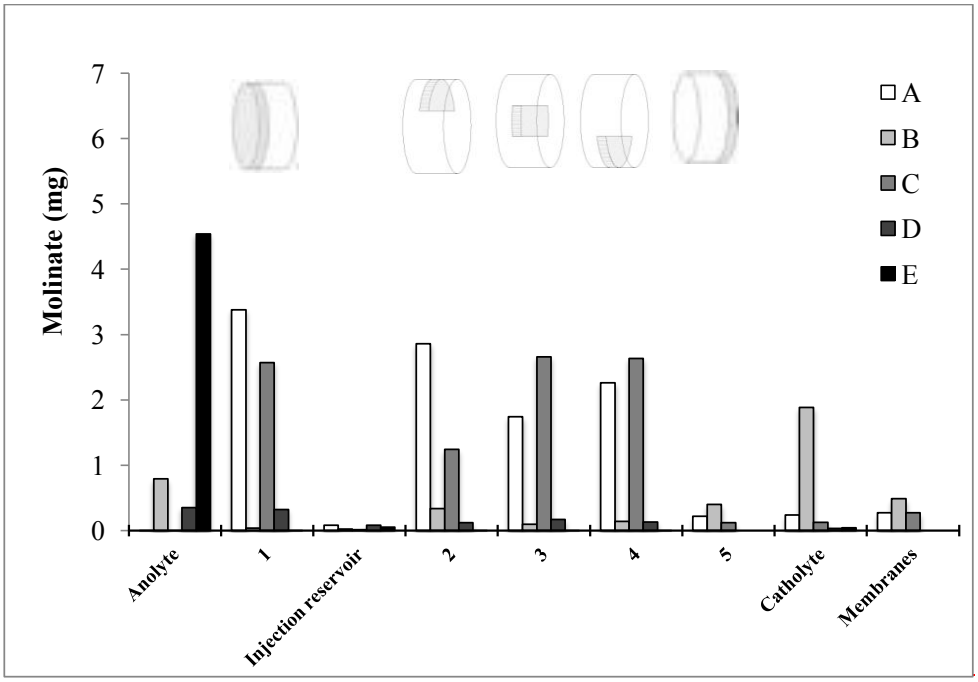

a) Experiments with soil 1 (sandy soil): B (EK with pH control) and E (diffusion);
b) Experiments with soil 2 (sandy loam with high organic matter content): A (EK without pH control), C (EK with pH control) and D (diffusion). In the diffusion experiments (D and E) higher molinate content was found in the anolyte due to the direct contact with the spiked soil.

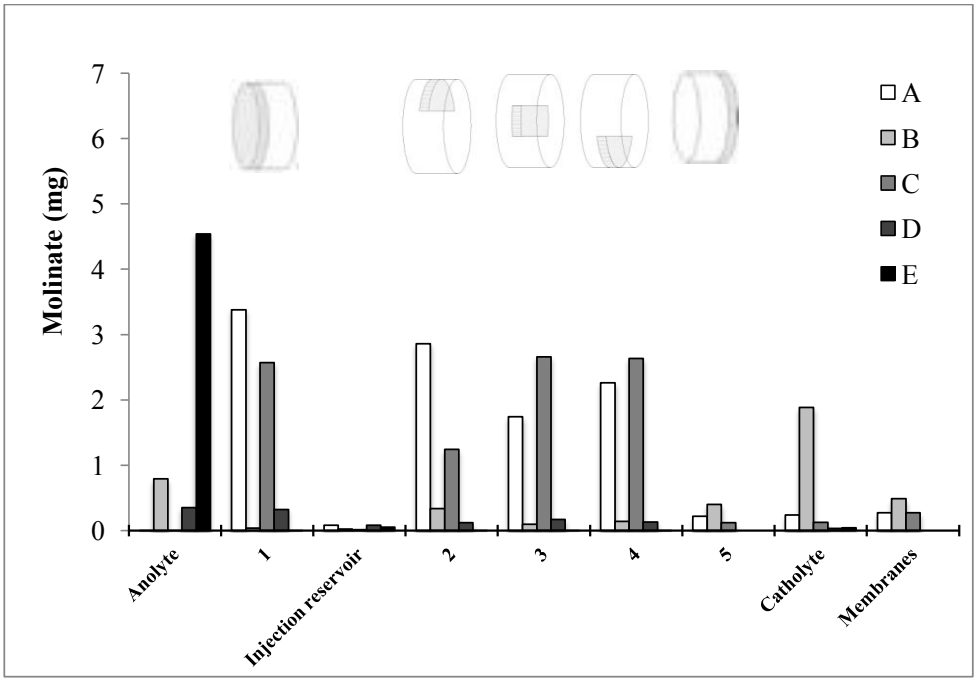

Figure 7. Mass of molinate in different compartments by the end of the experiments.

Table 1. Chemical and physical properties of molinate (Mabury et al., 1996).

Chemical Name	Molinate
CAS No.	2212-67-1
Structure	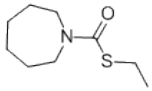
Molecular Formula	$C_9H_{17}NOS$
Boiling point	202°C (10 mm Hg)
Density	1.06
Water solubility	800-912 mg L^{-1}
Half-life	21 d
K_{oc}	190 mL g^{-1} OC
log K_{ow}	3.21

Table 2. Physical and chemical characteristics of the soils used.

Parameter	**S1**	**S2**
Textural classification	Sandy	Sandy loam
Organic matter (g kg^{-1})	4	128.3
pH (H_2O)	5.9	6.1
pH (KCl)	4.5	5.4
Exchangeable cations ($cmol_{(c)}$ kg^{-1})		
Ca^{2+}	0.34	16.18
Mg^{2+}	0.05	3.98
K^{+}	0.05	0.70
Na^{+}	0.04	0.18
Sum of exchangeable cations ($cmol_{(c)}$ kg^{-1})	0.48	21.04
Cation exchange capacity ($cmol_{(c)}$ kg^{-1})	1.39	23.38
Saturation (%)	35	90

Table 3. Summary of experimental conditions. The electrolyte used was 10^{-2} M $NaNO_3$ and the duration of the experiments was 6 days.

Exp.	Soil	Current (mA)	Soil - dry weight (g)	Molinate added to soil (mg)	pH Control
A	S2	10	321.46	51.2	No
B	S1	10	381.41	55.8	NaOH 1M added to anolyte
C	S2	10	344.31	52.7	NaOH 1M added to anolyte
D	S2	0	251.89	52.6	No
E	S1	0	387.42	52.6	No

Table 4. Molinate removal rate.

Experiment	Soil	Initial content in soils (mg)	Transported to the anode (mg)	Transported to the cathode (mg)	Final content in soils (mg)	Removal rate (%)
A	S2	51.2	0.004	0.237	10.46	72.3
B	S1	55.8	1.323	1.886	1.01	89.9
C	S2	52.7	0.003	0.125	9.22	71.2
D	S2	52.6	0.349	0.003	0.74	97.5
E	S1	52.6	4.540	0.044	0.00	91.3

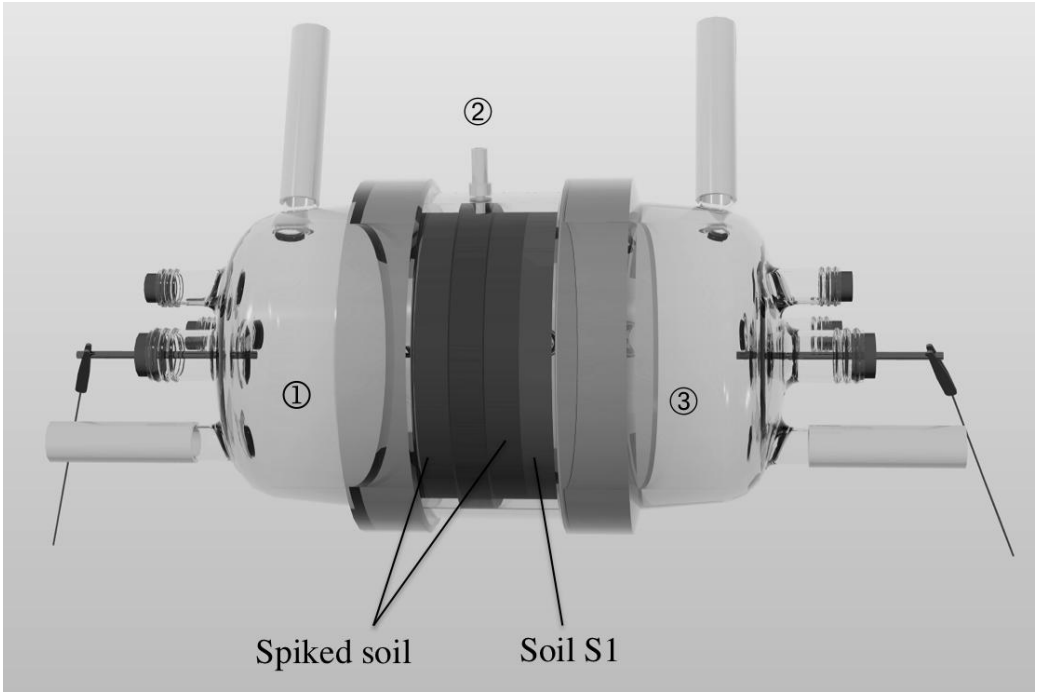

Figure 1. Schematic representation of the laboratory cell. Legend: ① Anode compartment; ② Reservoir for the iron nanoparticles injection; ③ Cathode compartment. The separation between the soil and the compartments containing liquids was made through passive membranes (filter paper).

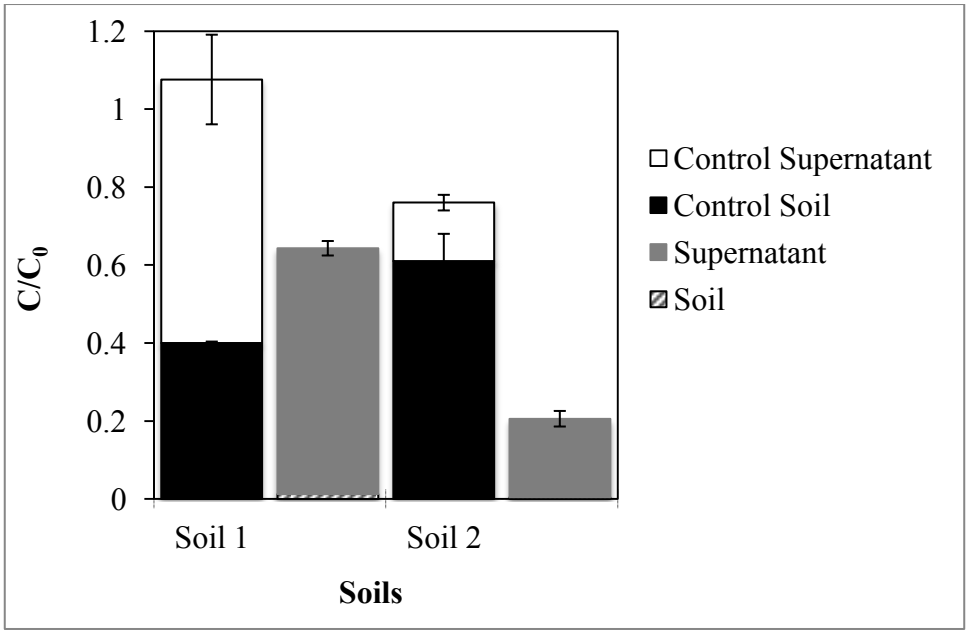

Figure 2. Molinate concentrations in the soil and supernatant after 24 h, with and without nZVI (control) in S1 sandy soil and S2 sandy-loam soil. Initial molinate concentration in soil was 290 mg kg^{-1}. Data plotted as mean of duplicates, error bars indicate standard deviation.

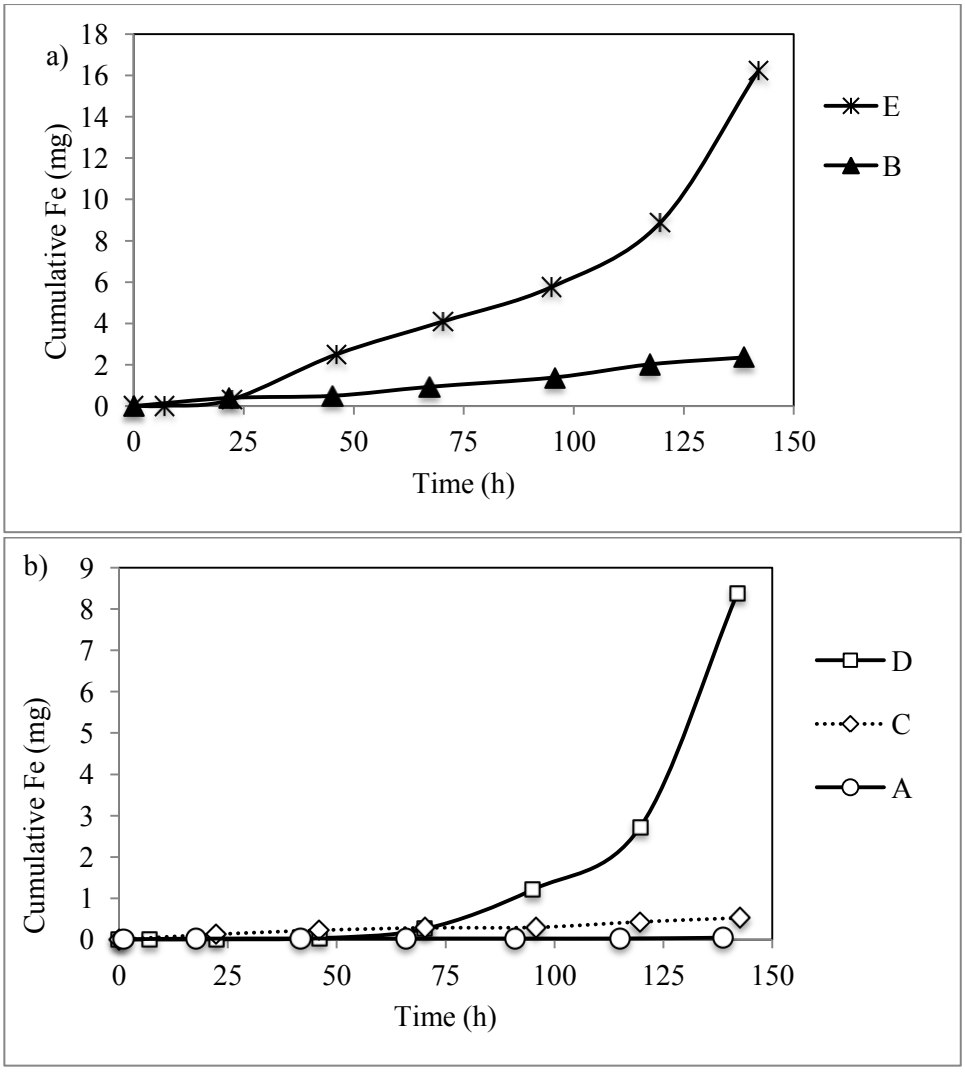

Figure 3. Cumulative amounts of total iron (mg) in the anolyte solutions during the experiments. a) Experiments with soil 1 (sandy soil): B (EK with pH control) and E (diffusion); b) Experiments with soil 2 (sandy loam with high organic matter content): A (EK without pH control), C (EK with pH control) and D (diffusion). In the cathode compartment, iron was detected in very low concentrations and in most of the samples was below the detection limit.

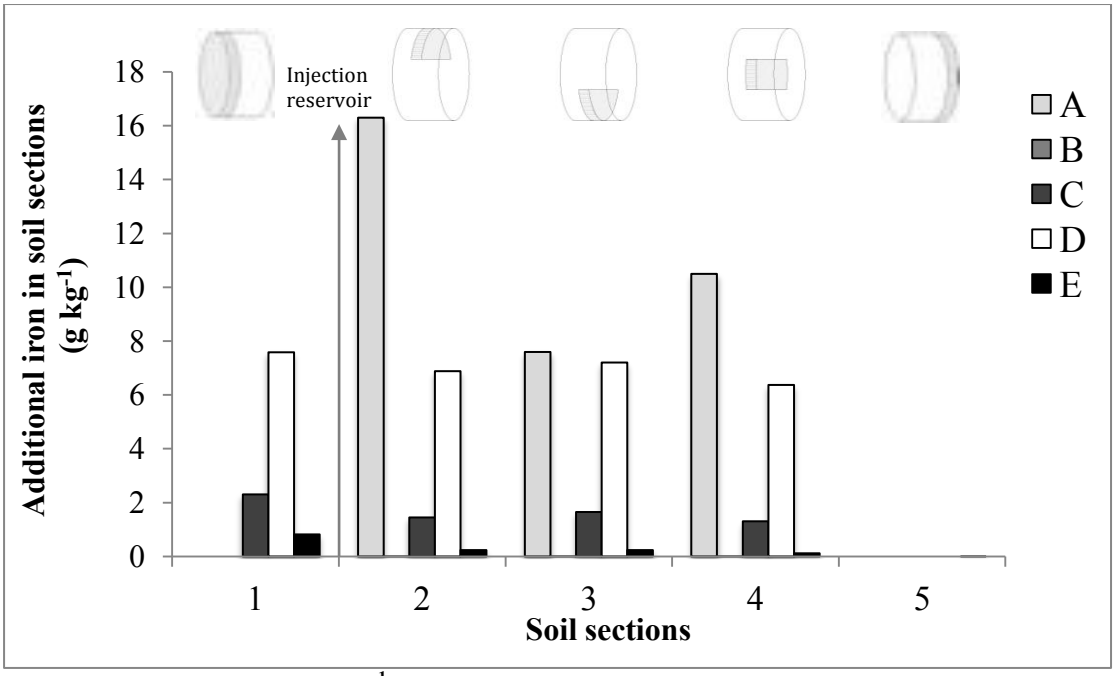

Figure 4. Iron enrichment (g kg^{-1}) in soil sections (compared to initial soil concentration: 18.43 g kg^{-1} in Soil S1 and 0.85 g kg^{-1} in Soil S2) in experiments A-E. Section 1: between the anode compartment and the injection reservoir; Section 2: central soil section after the injection reservoir, top; Section 3: central soil section after the injection reservoir, bottom; Section 4: central soil section after the injection reservoir, center; Section 5: between the central soil section and the cathode compartment.

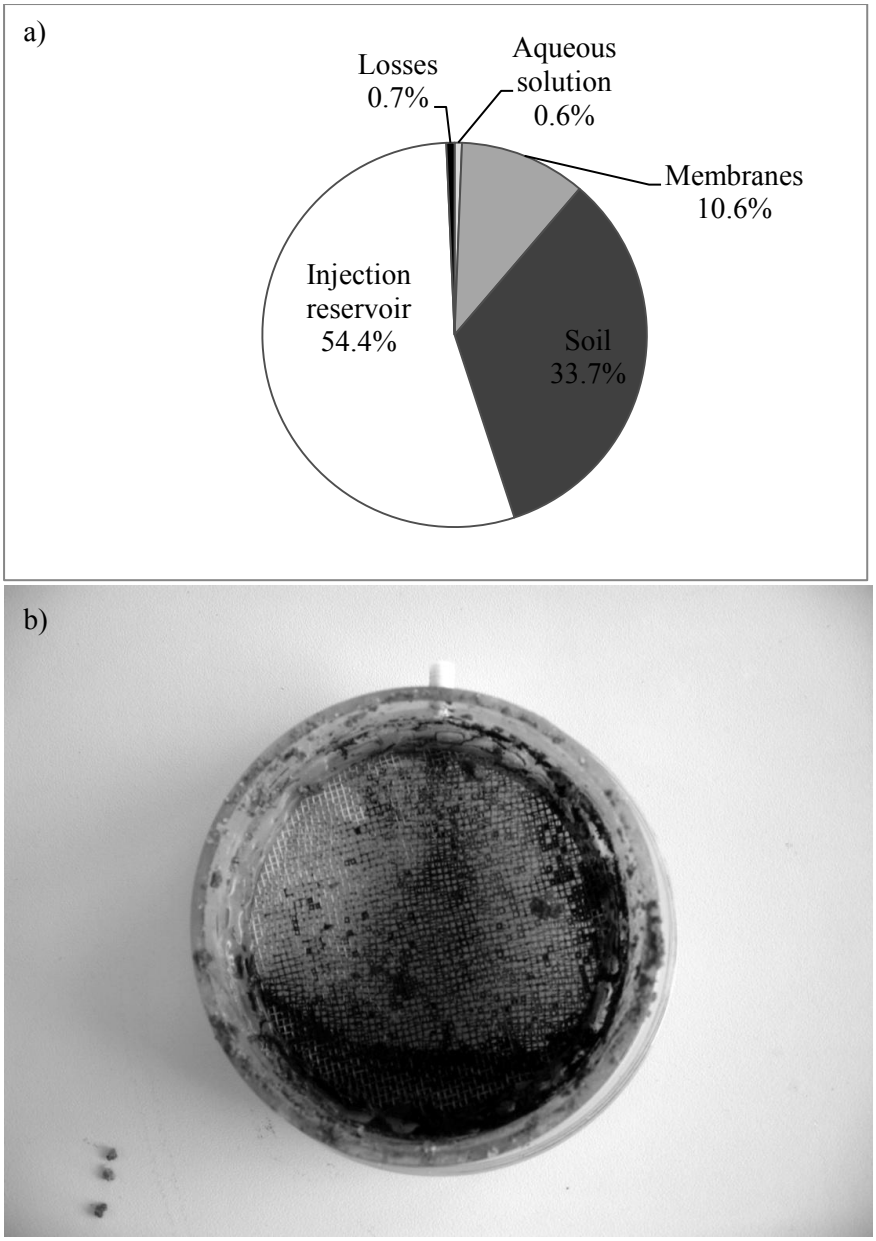

Figure 5. a) Average mass balance of iron after the experiments. Average recovery of iron was 86%. b) Photo of the experimental cell showing the iron accumulation in the injection reservoir.

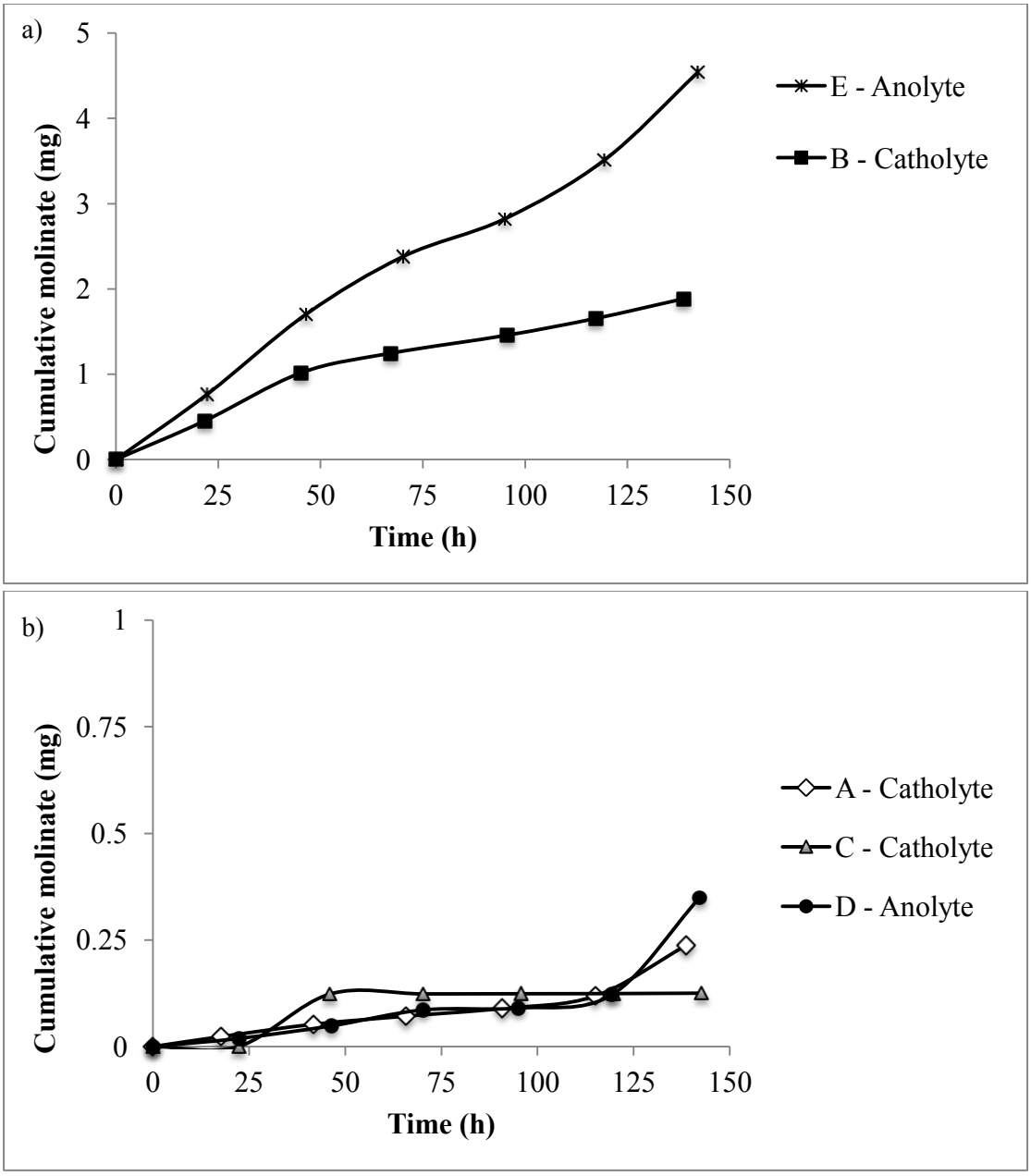

Figure 6. Cumulative amounts of molinate (mg) in the anolyte and catholyte solutions during the experiments.
a) Experiments with soil 1 (sandy soil): B (EK with pH control) and E (diffusion);
b) Experiments with soil 2 (sandy loam with high organic matter content): A (EK without pH control), C (EK with pH control) and D (diffusion). In the diffusion experiments (D and E) higher molinate content was found in the anolyte due to the direct contact with the spiked soil.

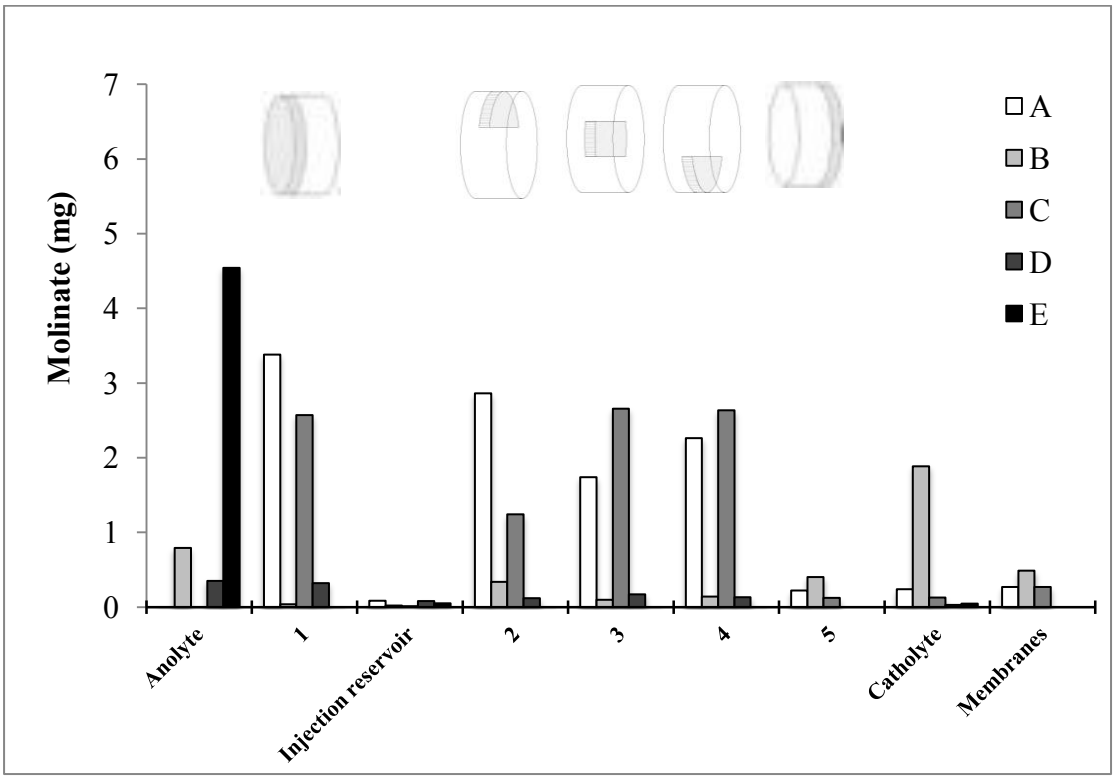

Figure 7. Mass of molinate in different compartments by the end of the experiments.